Palytoxin Induces Cell Lysis by Priming a Two-Step Process in MCF-7 Cells

ARTICLE *in* CHEMICAL RESEARCH IN TOXICOLOGY · AUGUST 2011

Impact Factor: 3.53 · DOI: 10.1021/tx2001866 · Source: PubMed

7 AUTHORS, INCLUDING:

Simone Prandi
Universität Potsdam
5 PUBLICATIONS **43** CITATIONS
SEE PROFILE

Mirella Bellocci
Università degli Studi di Modena e Reggio E…
11 PUBLICATIONS **130** CITATIONS
SEE PROFILE

Paolo Facci
Italian National Research Council
98 PUBLICATIONS **2,068** CITATIONS
SEE PROFILE

Albertino Bigiani
Università degli Studi di Modena e Reggio E…
50 PUBLICATIONS **1,143** CITATIONS
SEE PROFILE

Chemical Research in Toxicology

ARTICLE

pubs.acs.org/crt

Palytoxin Induces Cell Lysis by Priming a Two-Step Process in MCF-7 Cells

Simone Prandi,[†] Gian Luca Sala,[†] Mirella Bellocci,[†] Andrea Alessandrini,[‡,§] Paolo Facci,[‡] Albertino Bigiani,[†] and Gian Paolo Rossini*[,†]

[†]Dipartimento di Scienze Biomediche, Università di Modena e Reggio Emilia, Via Campi 287, I-41125 Modena, Italy

[‡]Center S3 of CNR-Institute of Nanoscience, Via Campi 213/a, I-41125 Modena, Italy

[§]Dipartimento di Fisica, Università di Modena e Reggio Emilia, Via Campi 213/a, I-41125 Modena, Italy

Supporting Information

ABSTRACT: The cytolytic action of palytoxin (PlTX) was recognized long ago, but its features have remained largely undetermined. We used biochemical, morphological, physiological, and physical tools, to study the cytolytic response in MCF-7 cells, as our model system. Cytolysis represented a stereotyped response induced by the addition of isotonic phosphate buffer (PBS) to cells that had been exposed to PlTX, after toxin removal and under optimal and suboptimal experimental conditions. Cytolysis was sensitive to osmolytes present during cell exposure to PlTX but not in the course of the lytic phase. Fluorescence microscopy showed that PlTX caused cell rounding and rearrangement of the actin cytoskeleton. Atomic force microscopy (AFM) was used to monitor PlTX effects in real time, and we found that morphological and mechanical properties of MCF-7 cells did not change during toxin exposure, but increased cell height and decreased stiffness at its surface were observed when PBS was added to PlTX-treated cells. The presence of an osmolyte during PlTX treatment prevented the detection of changes in morphological and mechanical properties caused by PBS addition to toxin-treated cells, as detected by AFM. By patch-clamp technique, we confirmed that PlTX action involved the transformation of the Na^+,K^+-ATPase into a channel and found that cell membrane capacitance was not changed by PlTX, indicating that the membrane surface area was not greatly affected in our model system. Overall, our findings show that the cytolytic response triggered by PlTX in MCF-7 cells includes a first phase, which is toxin-dependent and osmolyte-sensitive, priming cells to lytic events taking place in a separate phase, which does not require the presence of the toxin and is osmolyte-insensitive but is accompanied by marked reorganization of actin-based cytoskeleton and altered mechanical properties at the cell's surface. A model of the two-step process of PlTX-induced cytolysis is presented.

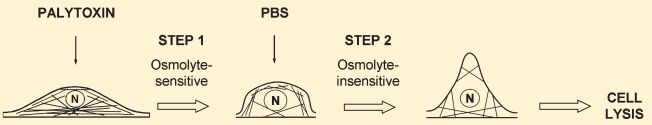

INTRODUCTION

Palytoxin-group toxins (PlTXs) are natural compounds which have been originally found in zoantharians of the genus *Palythoa*[1,2] and are produced by benthic microalgae of the genus *Ostreopsis*.[3−6] The structure of these compounds is characterized by the presence of a large hydrophilic polyether portion, containing many hydroxylic groups, and including a short lipophilic hydrocarbon chain in the first half of the molecule.[1,7−9]

PlTXs have been linked to episodes of human poisoning following the ingestion of the toxin with contaminated food and as a consequence of skin contact with contaminated marine aquarium zoanthids (reviewed in refs 10,11). The growth of *Ostreopsis* algae in warm waters had limited the occurrence of PlTX poisoning episodes to tropical areas in the past.[10] In the last 10 years, however, *Ostreopsis* blooms have appeared in coastal areas of Mediterranean countries with increasing frequency and distribution.[10,12,13] In several cases, these blooms have been accompanied by the intoxication of people on the seashore close to the waters where the algal blooms were taking place, leading to the proposal that symptoms had been caused by PlTXs present in aerosols[10,11,14] and raising novel concerns about the effects of PlTX on human health.

It has long been recognized that biological effects of PlTX stem from its property to bind to Na^+,K^+-ATPase on the plasma membrane, converting the pump into a nonspecific cation channel,[15] (see also the recent reviews in refs 16−18). The alteration of mechanisms responsible for Na^+ and K^+ homeostasis in cells is the recognized primary cause of adverse consequences of PlTX poisoning.[17−19] The excitable cells of the nervous and muscular systems are major targets of PlTX,[17,19] but the essentially ubiquitous distribution of Na^+,K^+-ATPase in animal cells is matched by the capacity of this toxin to alter a variety of processes in both excitable and nonexcitable cells,[17−19] leading to cell death in many experimental systems (reviewed in ref 20), and raising questions regarding the molecular bases of delayed effects and alterations of nonexcitable tissues (see ref 18 and references therein).

Received: May 4, 2011
Published: July 05, 2011

The hemolytic action of PlTX is one of the first effects described in nonexcitable cells, in the pioneering investigations by Habermann and his collaborators,[21] paving the way to the formal proof that the Na^+,K^+-ATPase is the molecular target of PlTX.[15] In their original study, the loss of K^+ ions from rat erythrocytes was observed within minutes from cell exposure to nanomolar concentrations of PlTX, and this response was followed by a hemolysis which was delayed by 1 h or longer with reference to the cellular loss of K^+ ions.[21]

The cytolytic effect of PlTX has been exploited to develop cell-based, functional assays for the detection and quantification of these toxins in naturally contaminated samples.[22−26] In the course of our activities to develop a cell-based functional assay for the detection and quantification of PlTX-group toxins in natural samples, we obtained some preliminary data on the lytic process in the human epithelial cell line MCF-7, which was triggered under controlled conditions.[23] In that experimental setting, cells were exposed to PlTX in an initial incubation, which was terminated by the removal of the culture medium, and cytolysis was then induced by the addition of a phosphate buffered saline solution to the cell monolayer and in the absence of toxin.[20,23] The capacity of an isotonic buffer to induce cell lysis had been already reported,[21] but the response is counterintuitive when framed by a model of osmotic lysis[21] and has attracted our attention.

In this investigation, we have integrated biochemical, morphological, physiological, and physical analyses to study the cytolytic response induced by PlTX in MCF-7 cells under controlled experimental conditions. The data we obtained show that the response involves a two-step process displaying specific features. The first step is toxin-dependent and osmolyte-sensitive, priming the cells to lytic events, which take place in a following phase that does not require the presence of the toxin and is osmolyte-insensitive but is accompanied by marked reorganization of the actin-based cytoskeleton and altered mechanical properties at the surface of MCF-7 cells.

MATERIALS AND METHODS

Materials. Palytoxin was obtained from Wako Chemicals (Germany). Stock palytoxin solutions (50 μM) were prepared in absolute ethanol, and their working dilutions were prepared in 60% ethanol. The toxin solutions described above were stored in glass vials protected from light at −20 °C. Trehalose, sorbitol, glycerol, L-proline, betaine, and ouabain were obtained from Sigma (Milan, Italy). The monoclonal anti-E-cadherin antibody was from Alexis (clone HECD-1) and the monoclonal antiactin antibody was obtained from Chemicon International. The 4′,6-diamidino-2-phenylindole dilactate (DAPI, dilactate) stain, fluorescent secondary antibody Alexa Fluor 468-conjugated antimouse IgG, and Oregon Green 488 phalloidin as well as Prolong Gold mounting media were from Invitrogen. All other reagents were of analytical grade.

Cell Culture Conditions. MCF-7 cells were obtained from European Collection of Animal Cell Cultures (ECACC No: 86012803) and were maintained in continuous culture, as previously described.[27]

Detection of Cytolysis. If not stated otherwise, cytolysis was analyzed using cells in logarithmic growth, which were seeded in 24 well (Ø 15 mm) plates, and the experiment was carried out the day after seeding, following the procedure we already described.[23] When the effect of osmolytes on cytolytic response was evaluated, individual osmolytes were dissolved in the culture medium at the concentrations specified under Results, to minimize possible dilutions of other components in the complete culture medium. In these cases, cell incubations were carried out after replacing the medium for cell culture with that for the experiment, which represented the complete culture medium added with the indicated concentrations of individual osmolytes, and cell samples were then preincubated for 15 min at 37 °C before receiving the addition of PlTX. If not stated otherwise, cell samples (0.6 mL/well) received either 0.3 nM PlTX or vehicle (60% ethanol) and were next incubated for 1 h at 37 °C. When cell incubations were carried out at temperatures other than 37 °C, cell samples were not maintained in an incubator and exposed to an atmosphere containing carbon dioxide. In these cases, 20 mM HEPES buffer, pH 7.2, was added to the culture medium to keep its buffering capacity throughout the treatment of cell samples. At the end of the incubations, the culture medium was disposed by suction, 0.5 mL of 20 mM phosphate buffer, pH 7.4, containing 0.15 M NaCl (PBS) were added to each well, and cells were then maintained for 1 h at 4 °C. In some experiments, the temperature of this second incubation was changed, as specified under Results.

In the standard procedure for the analysis of the cytolytic response, the buffer was retrieved from culture wells at the end of the incubation with PBS, yielding a culture supernatant that was used for the assay of lactate dehydrogenase (LDH) activity, according to Wróblewski and LaDue.[28] The assay of LDH activity was performed in a 96-well plate, and each well contained 20 μL of culture supernatant, in duplicate, and the enzymatic reaction was started by adding 180 μL of 52 mM phosphate buffer, pH 7.4, 0.18 mM NADH, and 0.63 mM sodium pyruvate. The absorbance at 340 nm was recorded by a plate reader at 1-min intervals, during the first 10 minutes of incubation at room temperature, and the LDH activity was expressed as the decrement of A_{340} per min.

Immunofluorescence Studies. When immunofluorescence microscopy was used, cells were grown in 35 mm Petri dishes containing one coverslip glass in each dish. Cells in logarithmic growth were treated for 1 h with indicated PlTX concentrations, or vehicle, and for 1 h with PBS, as described above. Cells were then fixed with 4% (w/v) paraformaldehyde in PBS for 15 min at room temperature. After fixation, cells were permeabilized by treatment with PBS buffer containing 3% (w/v) bovine serum albumin and 0.02% Triton X-100, for 1 h at room temperature. Samples were then incubated overnight at 4 °C with the indicated primary antibodies, which were diluted in PBS containing 1% BSA, at the final concentration indicated on the information sheet of the respective antibody. The incubations with fluorescent secondary antibodies were performed for 45 min at room temperature in the dark, using antibodies at a final 1:1000 dilution. In the case of F-actin labeling, cells, after permeabilization, were incubated with 165 nM Oregon green 488 phalloidin in PBS containing 1% BSA for 20 min at room temperature in the dark. Labeling of nuclei was obtained by cell incubation for 5 min with a 0.14 μg/mL DAPI solution in PBS. Cells were then mounted on microscopic slides using ProLong Gold (Invitrogen) mounting media and evaluated under a Zeiss Axioscop-40 microscope. Images were acquired by an AxioCam HRc camera (Carl Zeiss), using the Axiovision 3.1 software (Carl Zeiss).

Atomic Force Microscopy. MCF-7 cells were studied by atomic force microscopy (AFM) with a Bioscope AFM (Veeco Digital Instruments, USA) using triangular Si_3N_4 cantilever (Olympus). The spring constant of each cantilever was determined by the thermal noise method at the beginning of each experiment.[29] The cells were imaged in their culture medium at a temperature of 19 °C. The low temperature used in the experiments decreased the problems connected with evaporation in long imaging sessions (3−4 h), and preliminary experiments showed that this lowering of the temperature during the experiment slowed down the recorded responses without affecting their overall characteristics. In the course of this procedure, cell samples could not be exposed to an atmosphere containing carbon dioxide, and 20 mM HEPES buffer, pH 7.2, was added to the culture medium to keep its buffering capacity. Maps of the morphological and mechanical properties of the cells were obtained by the Force Volume approach.[30] Briefly, force-displacement

curves were obtained in a 64 × 64 two-dimensional matrix acquiring 64 points for each direction of the force curve (approach and withdrawn). For each force curve, the cantilever is moved toward the sample until a preset deflection set point is reached. The z-movement of the cantilever was 3.5 μm obtained at a vertical speed of 28 μm/s. Subsequently, the cantilever is withdrawn from the sample and moved to another pixel of the matrix to acquire another force curve. The set of obtained force curves can then be exploited to extract maps of both the Young's modulus and the zero-loading-force height of the cells. To extract this information, the Hertz model[31] was assumed to describe the relationship between the loading force and the cell indentation.[32] The Hertz model predicts the indentation value in the case of a stiff tip indenting a soft and flat sample. For the tip geometry, a cone with an opening angle of 35° was assumed. A plot of the indentation as a function of the applied force established that the conical model for the tip assured the best fitting to the data. The Poisson ratio, describing the ratio between the deformation in a direction perpendicular to the applied force and the deformation in the direction of the force, was assumed to be equal to 0.5. The analytical expression describing the relationship between the sample height and the cantilever deflection includes also the unknown offset of the sample height, which corresponds to the true height of the cell, not including the indentation due to the tip. By choosing two points along the force curve (two height values with the corresponding deflection values), it is possible to write a system of two equations which can be solved to give the corresponding Young's modulus and the zero-load height.[32] We assessed the dependence of the obtained Young's modulus on the particular choice of the two points along the force curve.[33] The values we obtained were largely independent of the selection of the points if an indentation greater than 200 nm was considered.

To test the effect of the different treatments on the cells, we first waited for the stabilization of mechanical and morphological cell properties as sensed by AFM. This step was necessary to avoid problems connected with temperature change from 37 to 19 °C, sustained by the cells passing from 37 °C (cell growth temperature) to 19 °C (temperature in AFM imaging conditions). In fact, it is known that a temperature decrease can induce an increase in the cell volume[34] and a consequent decrease in the Young's modulus.[35] The stabilization is usually achieved after 1 h. The medium exchange was obtained by a syringe pump at a flow rate which allowed the maintenance of a constant volume and temperature in the thermostatted imaging cell.

The data are reported as maps of the Young's modulus and zero-load height as a function of time during the different treatments to the cells. The time resolution of the measurement is limited by the time required for acquiring a force volume image (45 min). Even if this time period may appear too long to study rapid dynamic processes, it is compatible with the time periods used with the other techniques used in this work. The variations of the mechanical properties and of the volume are measured in the highest part of the cells to avoid interference from the underlying solid support. To circumvent the problems connected with the choice of the same position on the cell in image sequences, the morphological and mechanical properties were averaged on an area comprising nine force curves. The variations are reported in percentage terms with respect to the corresponding value at the end of the initial stabilization.

Electrophysiology. The patch-clamp technique[36] was used for the electrophysiological characterization of MCF-7 cells. Cells were seeded at a density of 2×10^4 cells/cm^2 on coverslips (Ø 14−15 mm) placed in 35-mm-Petri dishes 24 h prior to recording. On the day of the experiments, the coverslip was transferred into a recording chamber, consisting of a standard glass slide onto which a silicone ring 1−2 mm thick and 17−18 mm of inner diameter was pressed.

Membrane currents of a single MCF-7 cell were studied at room temperature (20−25 °C) by a whole-cell patch clamp using an Axopatch 1D amplifier (Axon Instruments, Union City, CA). Signals were recorded and analyzed using a Pentium computer equipped with a Digitada 1320A data acquisition system and pClamp10 software (Axon Instruments). pClamp10 was used to generate voltage-clamp commands and to record the resulting data. Signals were prefiltered at 10 kHz and digitized at 10-μs intervals. MCF-7 cells were stimulated by applying a series of 20-ms depolarizing pulses (voltage steps), in 10-mV increments, from a holding potential of −50 mV.[37]

Patch pipettes were made from borosilicate glass capillaries (Garner Glass, Claremont, CA) on a 2-stage vertical puller (model PP-830, Narishige, Tokyo, Japan). Typical pipet resistances were 2−5 MΩ when filled with intracellular solution.

The intracellular solution in the recording pipet contained 150 mM KCl, 2 mM $MgCl_2$, 10 mM HEPES, and 1.1 mM EGTA, pH 7.2, adjusted with KOH.[38] Cells were bathed with an external solution containing 140 mM NaCl, 5 mM KCl, 2 mM $CaCl_2$, 2 mM $MgCl_2$, 10 mM HEPES, and 5 mM glucose, pH 7.4, adjusted with NaOH.[38] For electrophysiological experiments, dilutions of PlTX 300 nM were used and stored at −20 °C. The toxin was diluted the day of the experiments in a nonmodified external solution to a final concentration of 0.1 nM. Ouabain was dissolved the day of the experiments in a nonmodified external solution to the final concentration of 100 μM.

Gravity-fed test solutions were controlled by multisolenoid manifold valves and introduced through a common inlet into the recording chamber. Most data analyses were performed using pClamp10. Additional analysis was performed using Microsoft Excel and Prism 3.03 software (Graph Pad Software, San Diego, USA) for plotting. Results are presented as the means ± standard error of the mean.

Cell membrane capacitance (C_m) was calculated with the following equation (modified from ref 39):

$$C_m = \frac{\tau \cdot I_0}{\Delta V \cdot (1 - I_{SS}/I_0)}$$

where τ is the exponential decay of the capacitive transient, I_0 is the current amplitude at the beginning of the voltage step (time 0), ΔV represents the voltage step from the holding potential (10 mV), and I_{SS} is the steady-state value of the current at the end of the voltage step. Input resistance (R_{in}) was evaluated as slope resistance of the current−voltage ($I-V$) relationship at the holding potential of −50 mV.

The permeability to Na^+ relative to that of K^+ (P_{Na}/P_K) was calculated using the Goldman−Hodgkin−Katz equation:[40]

$$E_{rev} = \frac{R \cdot T}{F} \cdot \log_{10} \frac{[K]_{ext} + \frac{P_{Na}}{P_K} \cdot [Na]_{ext}}{[K]_{int} + \frac{P_{Na}}{P_K} \cdot [Na]_{int}}$$

where E_{rev} is the current reversal potential from the current−voltage relationship ($I-V$), R is the gas constant, F the Faraday constant, T the temperature, $[K]$ and $[Na]$ the potassium and sodium concentrations (int, intracellular; *ext*, extracellular), respectively, and P_K and P_{Na} the membrane permeabilities to potassium and sodium, respectively.

Quantification of Data. Data analyses were performed as detailed in the individual sections above. Student's *t* test was used to evaluate the significance of the experimental data.

RESULTS

Effect of Osmolytes on the Cytolytic Response Induced by Palytoxin in MCF-7 Cells. Preliminary experiments were carried out to check the dose−response curve of PlTX-induced cytolysis of MCF-7 cells. The data we obtained confirmed our previous observations,[23] and showed that a maximal cytolytic effect could be detected at PlTX concentrations higher than 0.2 nM, under our experimental conditions (Figure S1, in Supporting Information). In the following experiments,

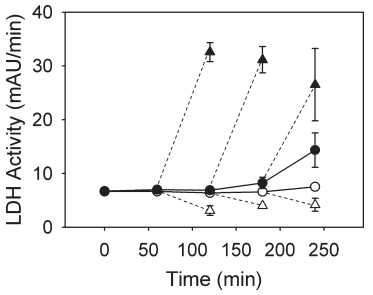

Figure 1. Cytolytic effect triggered by palytoxin in MCF-7 cells. Cells grown as a monolayer in complete culture medium received 0.3 nM PlTX (closed symbols) or vehicle (open symbols) and were incubated at 37 °C. At the indicated times, the medium bathing the cells was removed and used for the analysis of LDH activity (circles, solid lines), as described under Materials and Methods. The cells remaining in culture wells received the addition of PBS buffer devoid of toxin, and the incubation was continued for 1 h at 4 °C. At the end of this incubation, PBS bathing the cells was removed and used for the analysis of LDH activity (triangles, dashed lines), as described under Materials and Methods. Data represent the means ± SD obtained from quadruplicate samples in two separate experiments.

therefore, the cytolytic response was induced in MCF-7 cells by exposure to either optimal (0.3 nM) or suboptimal (0.1 nM) PlTX concentrations, as specified in the text.

In previous studies, we showed that the addition of PBS to MCF-7 cells induced cytolysis in samples which had been exposed to PlTX for 1 h at physiological temperature.[20,23] In those studies, however, we did not establish to what extent the cytolytic events were a direct consequence of PBS addition to toxin-treated cell monolayers or might have resulted primarily from the kinetics of a cell death response induced by PlTX under our experimental conditions and independently of PBS addition. This aspect was then ascertained by exposing MCF-7 cells to PlTX for different times and measuring the release of LDH activity in culture supernatants before and after the addition of PBS. The results are reported in Figure 1 and show that basal levels of LDH activity were detected in the culture medium bathing the cells in both control and PlTX-treated samples in the first 2 h of incubation at 37 °C, representing the enzyme originating from the serum added to the complete culture medium during the incubation of MCF-7 cells.[20] Increased levels of LDH activity, however, were detected in the culture medium bathing PlTX-treated, but not control cells, when incubations were carried out for 3 h and increased for a longer cell exposure to PlTX at 37 °C (Figure 1), confirming that prolonged exposure of MCF-7 cells to 0.3 nM PlTX is needed to detect cell destruction in culture dishes.[41] When culture medium was removed and cells received the addition of PBS, LDH activity was released in the buffer bathing the cells that had been exposed to PlTX at any time-point, whereas removal of contaminating LDH activity was attained in control cultures (Figure 1), confirming the conclusion that the LDH activity detected in the medium bathing PlTX-treated cells resulted from MCF-7 cell lysis induced by PBS addition.[20,23] Similar results were obtained in other experiments if the presence of cytosolic proteins other than LDH, but not plasma membrane proteins, in culture supernatants was checked by immunoblotting (Figure S2, in Supporting Information). The cytolysis we detected in MCF-7 cells, therefore, is a stereotypical response induced by the addition of PBS to cells exposed to PlTX and does not simply result from already ongoing lytic events occurring in cells that had been exposed to the toxin under our experimental conditions.

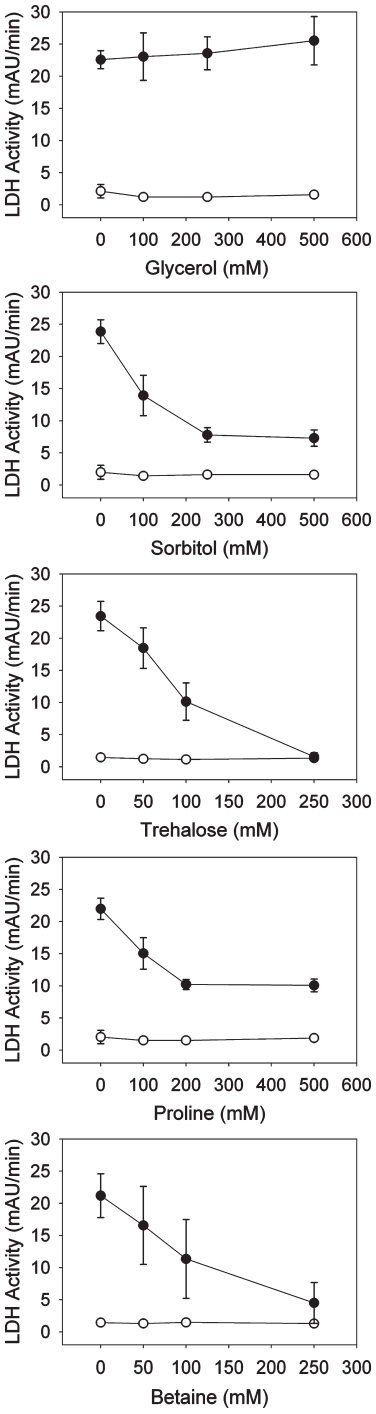

Figure 2. Effect of cell pretreatment with osmolytes on the cytolytic effect induced by palytoxin in MCF-7 cells. Cells were preincubated with complete culture medium containing the indicated concentrations of osmolytes for 15 min at 37 °C, before being treated with either 0.3 nM PlTX (●) or vehicle (○) for 1 h at 37 °C. At the end of the incubation, the culture medium was removed, and cell lysis was induced by PBS addition and cell incubation for 1 h at 4 °C. The measurement of LDH activity in culture supernatants was carried out, as described under Materials and Methods. Data represent the means ± SD obtained in three-four separate experiments.

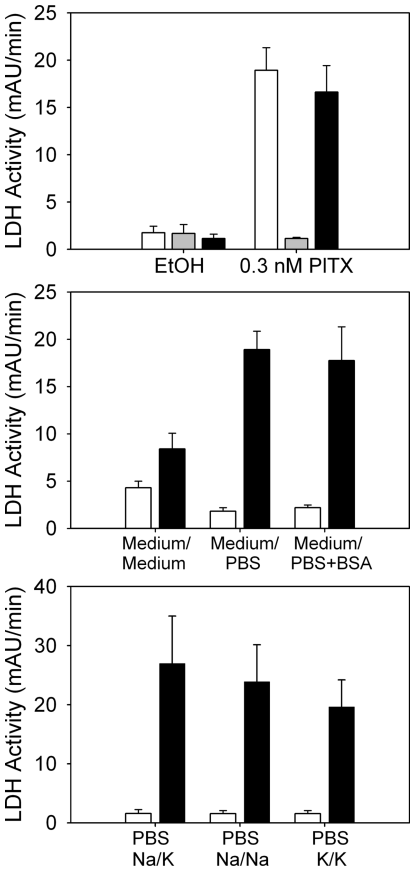

Figure 3. Effect of osmolyte composition of incubation medium on the cytolytic effect induced by palytoxin in MCF-7 cells. (Upper panel) Cells were preincubated with complete culture medium containing (gray bars) or lacking (black and open bars) 250 mM trehalose for 15 min at 37 °C, before receiving the addition of PlTX (0.3 nM) or vehicle (EtOH), as indicated. Cells were then incubated for 1 h at 37 °C, and at the end of the incubation, the culture medium was removed, and cells were exposed to PBS, either containing (black bars) or lacking (gray and open bars) 250 mM trehalose for 1 h at 4 °C. Cells were next processed for the measurement of LDH activity in culture supernatants, as described under Materials and Methods. Data represent the means ± SD obtained in three separate experiments. (Middle panel) Cells were incubated with either 0.3 nM PlTX (black bars) or vehicle (open bars) for 1 h at 37 °C. At the end of the incubation, the culture medium was removed, and cells were then exposed to fresh culture medium (medium/medium), PBS buffer (medium/PBS), or PBS buffer containing 3.8 mg/mL bovine serum albumin (medium/PBS + BSA), a protein concentration comparable to that contributed by fetal calf serum. Cells were next incubated for one additional h at 4 °C, before being processed for the measurement of LDH activity in culture supernatants, as described under Materials and Methods. Data represent the means ± SD obtained in four-seven separate experiments. (Bottom panel) Cells were incubated with either 0.3 nM PlTX (black bars) or vehicle (open bars) for 1 h at 37 °C. At the end of the incubation, the culture medium was removed, and cells were then exposed to phosphate buffer prepared by mixing dibasic sodium phosphate and monobasic potassium phosphate containing 150 mM NaCl (PBS Na/K), dibasic sodium phosphate and monobasic sodium phosphate containing 150 mM NaCl (PBS Na/Na), and dibasic potassium phosphate and monobasic potassium phosphate containing 150 mM KCl (PBS K/K). Cells were next incubated for one additional hour at 4 °C, before being processed for the measurement of LDH activity in culture supernatants, as described under Materials and Methods. Data represent the means ± SD obtained in four separate experiments.

It is known that the osmotic pressure of the medium bathing the cells during PlTX treatment affects their lytic responses.[21] We then probed the effect of osmotically active substances on the cytolytic response induced by PlTX in MCF-7 cells. The compounds we have chosen comprised the alditol sorbitol, the disaccharide trehalose, the amino-acids L-proline, and betaine, while glycerol was used in control samples, representing a cell membrane diffusible alditol.[42,43] Under our experimental conditions, the cytolysis triggered by PlTX treatment and induced by PBS addition was prevented if membrane impermeant osmolytes were present in the culture medium during cell exposure to the toxin (Figure 2). The protective effect of the osmolyte treatment was dose-dependent, and the efficacy of osmolytes followed the order trehalose > betaine > sorbitol ≥ L-proline, under our experimental conditions.

We next checked whether trehalose, which provided the best protection of MCF-7 cells to cytolysis during PlTX treatment under our experimental conditions, could prevent cell lysis when added after the removal of the toxin, being present in the incubation medium used during the second part of cell treatment (i.e., PBS). The results we obtained show that the protective effect of trehalose is lost if it is added to the cells after they had been exposed to PlTX (Figure 3, top panel).

On the basis of these findings, we then evaluated the influence that other experimental conditions during the second incubation may have on the cytolytic response induced by a previous cell treatment with PlTX. The results we obtained show that the use of the culture medium during the second incubation partially protects MCF-7 cells from cytolysis (Figure 3, middle panel). The protective effect of the culture medium was not simply due to the protein contributed by fetal calf serum, however, as the addition of BSA to the PBS buffer used in the second MCF-7 cell incubation did not protect them from the cytolysis induced by the prior treatment with PlTX (Figure 3, middle panel). These results implied that the composition of the medium bathing the cells during the second part of the incubation, after the removal of the culture medium, has a role in determining cell lysis. On the basis of the key role played by Na^+ and K^+ ions in the induction of cytolytic responses by PlTX,[21] we determined whether the effect of the toxin in our experimental system might depend on the presence of these ions in the medium added to the cells after toxin removal and we found that cell lysis could be induced when cells were exposed to either Na^+ or K^+-free isotonic buffers (Figure 3, bottom panel), implying that the occurrence of cytolysis in cells exposed to PlTX is not Na^+- or K^+-dependent after the toxin has been removed.

The hemolytic effect of PlTX has been shown to be temperature-sensitive.[21,25] The effect of temperature was then checked in our experimental model, and we found that MCF-7 cell lysis in cells that had been exposed to PlTX occurs at temperatures comprised between 4 and 37 °C, provided that the process is not prevented by the presence of trehalose during cell exposure to PlTX (Figures S3 and S4 in Supporting Information). The results we obtained, therefore, showed that the PBS-induced cytolysis in cells exposed to PlTX occurs at both physiological and non-physiological temperatures.

Overall, these results confirmed that the cytolytic effect induced by PlTX stems from altered ion homeostasis and that cytolysis can be counterbalanced by increased concentrations of osmolytes in the incubation medium during cell exposure to the toxin.[21] Furthermore, the results we obtained showed that the cytolytic response induced by PlTX in MCF-7 cells takes place in

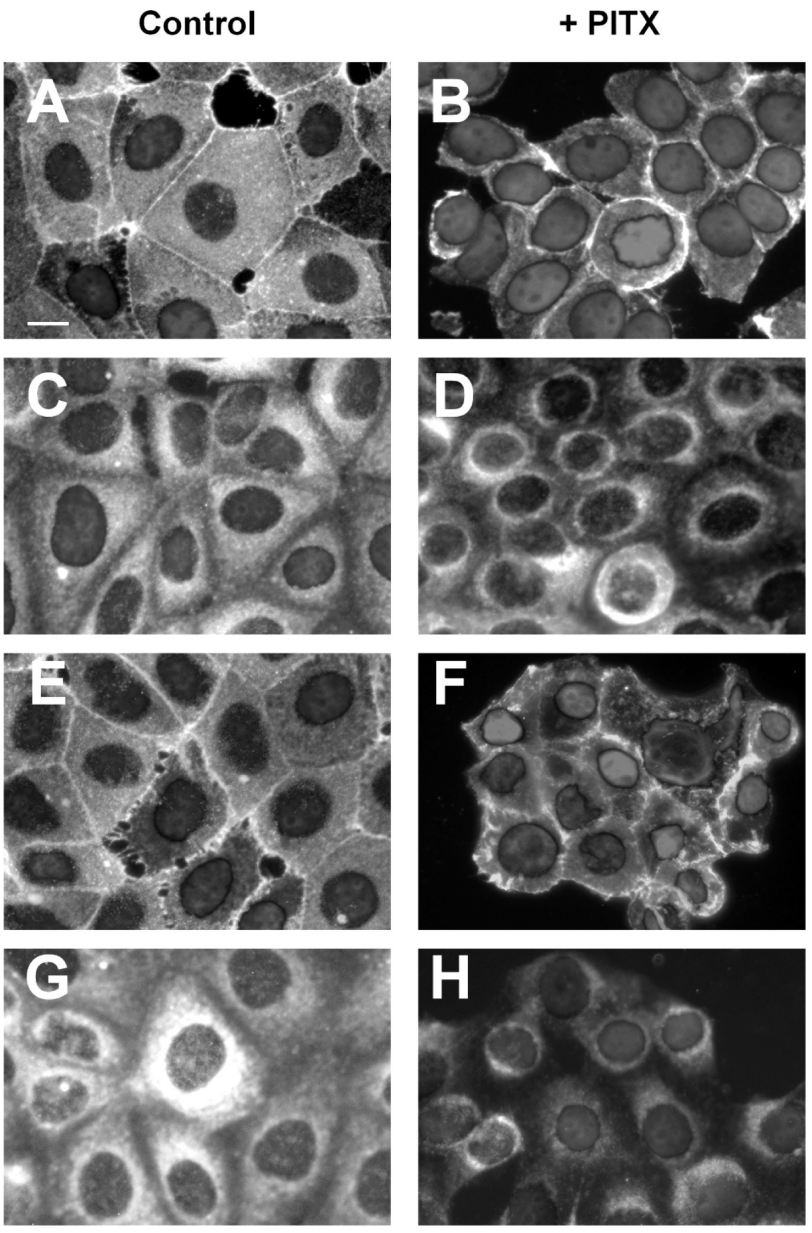

Figure 4. Effect of palytoxin on E-cadherin and actin-based cytoskeleton in MCF-7 cells. Cells were incubated with either 0.3 nM PlTX or vehicle, for 1 h at 37 °C, as indicated. At the end of the incubation, the culture medium was removed, and cells were either immediately processed for analysis by immunofluorescence microscopy (panels A−D) or received the addition of PBS, and the incubation was continued for one additional hour at 4 °C, before cells were processed for analysis by immunofluorescence microscopy (panels E−H), as described under Materials and Methods. Micrographs show the merging of the nuclear DAPI staining with the emissions of fluorescent secondary antibodies in cells that had been previously exposed to primary antibodies recognizing E-cadherin (panels A, B, E, and F) and actin (panels C, D, G, and H). The scale bar indicated in panel A corresponds to 10 μm and applies to all micrographs.

two steps, the first of which is toxin-dependent, osmolyte-sensitive, and is affected by the temperature of incubation, priming the cells to lytic events, which take place in a following phase. The lytic step does not require the presence of the toxin, is independent of the availability of extracellular Na^+ and K^+ ions, is not prevented by increasing osmolyte concentrations of the medium bathing the cells, and is marginally affected by temperature. These data, therefore, showed that PlTX induces a cytolytic response in MCF-7 cells under both optimal and suboptimal conditions, thereby allowing the study of the process by simple manipulations of basal experimental parameters.[21,25]

Analysis of MCF-7 Cells Exposed to Palytoxin by Immunofluorescece Microscopy. The data we obtained on the effect of osmolytes on the response triggered by PlTX in MCF-7 cells indicated that cell lysis induced by PBS in the second part of the incubation should not involve significant alterations of water movements and, consequently, should not be accompanied by gross changes in the morphological properties of MCF-7 cells. To gain further information onto this aspect, we then directly analyzed the effects of PlTX on the morphological properties of MCF-7 cells by the use of immunofluorescent probes and preliminarily assessed their apparent size and shape under the

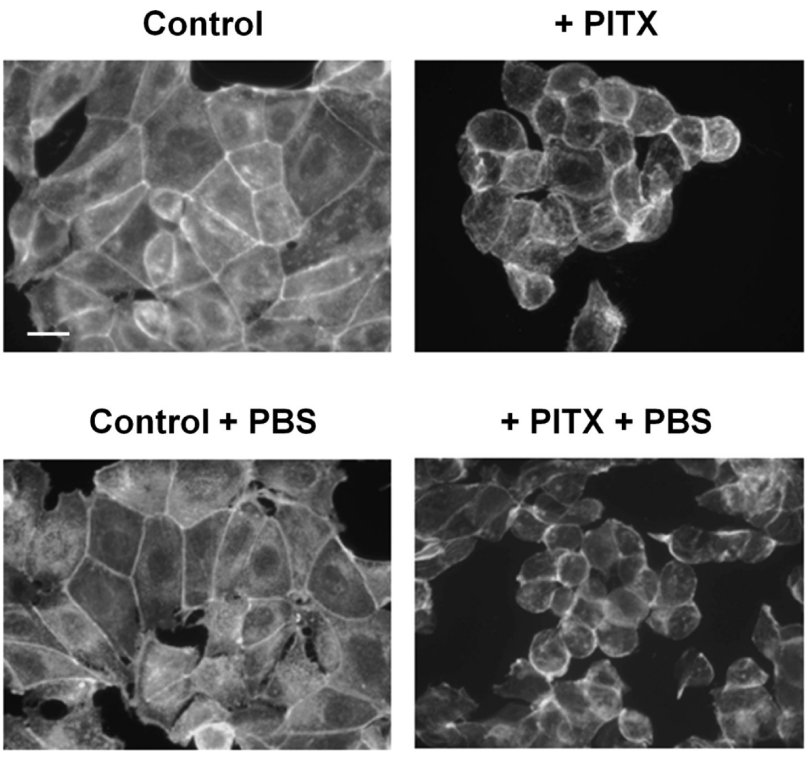

Figure 5. Effect of palytoxin on F-actin in MCF-7 cells. Cells were incubated with either 0.3 nM PlTX or vehicle, for 1 h at 37 °C. At the end of the incubation, the culture medium was removed, cells received the addition of PBS, and the incubation was continued for one additional hour at 4 °C, as indicated, before cells were processed for analysis by immunofluorescence microscopy, using Oregon-green phalloidin. The scale bar indicated in panel A corresponds to 20 μm and applies to all micrographs.

conditions of the present study. Two antibodies were used in these analyses, comprising an antiactin antibody, to visualize the actin-based cytoskeleton, and an anti-E-cadherin antibody, to detect the cell contours through an antibody bound to the plasma membrane protein responsible for cell−cell adhesion in epithelia.[44,45] MCF-7 cells were then treated with secondary antibodies tagged with a fluorescent moiety to visualize the cellular structures associated with the primary antibody. The results we obtained in a typical experiment are summarized in Figure 4, which reports the merging of the DAPI nuclear staining and the emission of fluorescent secondary antibodies used to detect our ultrastructural biomarkers. The exposure of cells to PlTX was found to result in limited ultrastructural changes at the end of the first hour of incubation with the toxin under our experimental conditions. The staining we obtained by the anti-E-cadherin antibody indicated that PlTX treatment caused a decrease in the cross-sectional area of PlTX-treated cells, as compared to that of the controls (Figure 4, compare panels A and B). The immunostaining obtained with the antiactin antibody confirmed this finding and indicated that the actin-based cytoskeleton was mostly concentrated in the peri-nuclear area of cells exposed to PlTX (Figure 4, compare panels C and D). When the culture medium was removed and cell incubation was continued for 1 more hour in the presence of PBS, no further changes in cellular ultrastructures were apparent (Figure 4, panels E−H) in addition to the large decrease in the number of cells still detectable in our cultures, as a consequence of extensive cell lysis during this second part of the incubation (see images we obtained at low magnification in Figure S5, in Supporting Information).

The indication that PlTX treatment induced a decrease in the cross-sectional area of MCF-7 cells and a relative reorganization of the actin-based cytoskeleton in the peri-nuclear region was further analyzed by semiquantitative estimates. The changes in the surface shape of the cells was probed by calculating the ratios of the major and minor diameters in individual cells, as detailed in Figure S6 of Supporting Information, and we found that PlTX treatment induced cell rounding (Figure S7 in Supporting Information). The apparent reorganization of the actin-based cytoskeleton in the peri-nuclear region of cells exposed to PlTX, in turn, was analyzed by quantifying the overall luminosity in fields possessing the same size in coverslips from control and PlTX-treated samples of MCF-7 cells. The results we obtained showed that PlTX treatment led to a marked decrease in the green emission detected in identical areas of analyzed fields, as compared to that of the controls (Figure S8, in Supporting Information), confirming the existence of a different cellular distribution of actin immunoreactivity in PlTX-treated, as compared to that of normal cells.

The use of antiactin antibodies did not allow us to distinguish between polymerized and globular actin in previous experiments with MCF-7 cells (Figure 4). As PlTX has been shown to induce a decrease in polymerized F-actin, with a concomitant increase of G actin subunits toward the nuclear region,[46] we checked our results with fluorescent phalloidin, which interacts with F-actin alone.[47] On the basis of the light emission of our fluorescent probe, the results we obtained revealed that the F-actin fibers were concentrated at the cell's periphery in PlTX-treated cells (Figure 5) so that the increased immunostaining detected by antiactin antibody in the peri-nuclear region (Figure 4) should

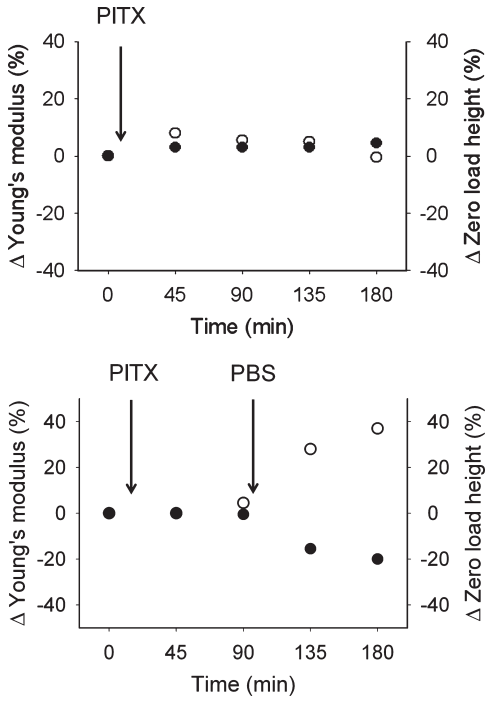

Figure 6. Effect of palytoxin on mechanical properties of MCF-7 cells by AFM. (Upper panel) Cells were incubated with 0.3 nM PlTX at 19 °C, and the percentage variation of the zero load height (empty symbols) and Young's modulus (closed symbols) were measured. The vertical arrow represents the time of PlTX injection. (Bottom panel) AFM analysis of MCF-7 cells exposure to PBS after treatment with palytoxin. Cells were incubated with 0.3 nM PlTX for 90 min at 19 °C. At the end of this incubation, the medium exchange for PBS started and the incubation continued at 19 °C. The vertical arrows represent the beginning of indicated treatments. Plot of the percentage variation of the zero load height (empty symbols) and Young's modulus (black symbols). The data result from an average of five cells for each time-point.

represent G actin. These findings, therefore, confirmed that PlTX induced a reorganization of the actin-based cytoskeleton.

Atomic force microscopy analyses of MCF-7 cells exposed to palytoxin. The data obtained by microscopic analysis of MCF-7 cells using immunofluorescent probes provided information on our model system at distinct time points of the experiments, but very limited insight became available into the dynamics of the morphological changes we detected in the course of cell treatments. To better characterize the changes in morphological and mechanical properties induced by PlTX during its action on MCF-7 cells in real time, we then used AFM, which represents a powerful tool to study the response of cells to chemical and pharmacological agents affecting their mechanical and morphological properties by time-lapse microscopy.[48−51] The elastic properties of an object can be described by the ratio between the applied mechanical stress, which is given by the force applied per unit area, and the resulting strain, which represents the deformation of the object normalized to its initial size. This ratio is the Young's modulus (E) of the object: the higher the Young's modulus, the stiffer the material. Even if an absolute quantitative evaluation of the Young's modulus of a cell by AFM presents many uncertainties, it is recognized that the relative variation of this parameter has a marked biological significance.[52,53]

The experimental procedures used in these experiments require prolonged times to acquire data from cellular samples. To minimize the chance that our experimental system might collapse during AFM analysis, we took advantage of the findings that the process under study can be depressed by cell treatments at lower temperatures (Figures S3 and S4 in Supporting Information). A first experiment was then carried out to asses the long-term stability of the Young's modulus of MCF-7 cells under basal conditions. MCF-7 cells were imaged in force volume mode at a constant temperature of 19 °C for 135 min. The typical value for the Young's modulus of MCF-7 cells was 1.5 ± 0.2 kPa, in reasonable agreement with previous measurements on the same type of cells.[54] Figure S9 (in Supporting Information) shows the behavior of the Young's modulus and of the cell height during a control experiment, expressed as percentages of the initial values (after the thermal stabilization), showing small variations of the Young's modulus and of the cell height over the course of our experiment.

Then we studied the effect of 0.3 nM PlTX on MCF-7 cells. The upper panel of Figure 6 (the corresponding cell images are reported in Figure S10 in Supporting Information) shows that marginal changes were detected in the Young's modulus and cell height as a consequence of cell exposure to PlTX under our experimental conditions. The cytolytic effect induced by the addition of PBS to PlTX-treated MCF-7 cells was next analyzed by AFM. To this end, we performed an experiment in which the cells were exposed to PlTX for 90 min, and then the imaging medium was exchanged for PBS. The bottom panel of Figure 6 (the corresponding cell images are reported in Figure S11 in Supporting Information) reports the behavior of the cells upon this treatment. As in the previous case, the exposure to PlTX does not significantly affect the morphological and mechanical properties of the cells. However, if the imaging medium is exchanged for PBS, a rapid increase of the cell height and a decrease of the Young's modulus is observed (Figure 6, bottom panel). It is important to stress that in a control experiment in which cells not previously exposed to PlTX undergo a medium exchange for PBS the morphological and mechanical parameters do not vary significantly (not shown). In keeping with the results we obtained by analysis of PlTX-induced cell lysis, these data indicated that the toxin might induce a latent damage to the cells which is amplified by PBS addition. On the basis of calculations using parameters of cell shape recorded in the course of AFM analysis, the increase in cell height was accompanied by a limited (30−50%) increase in cell volume. This change occurred in a phase that is not sensitive to osmolytes (Figure 3) and should not represent a direct consequence of an osmotic stress but would be due to a relative change in cell architecture. Indeed, the exposure of PlTX-treated MCF-7 cells to PBS in the second part of the incubation was accompanied by changes in mechanical properties at the cell surface, and a decrease in stiffness (Young's modulus) occurred. The relative change of cell shape we detected by AFM is in line with the decrease in the apparent cell diameter of cells treated with PlTX and then exposed to PBS, which we detected by immunofluorescence (Figures 4 and S7 in Supporting Information).

AFM was used in other experiments aimed at a better characterization of morphological and dynamic properties of MCF-7 cells exposed to trehalose. A preliminary experiment was carried out to evaluate the changes of the Young's modulus and cell height of MCF-7 cells when they were exposed to a culture medium containing increasing concentrations of the osmolyte.

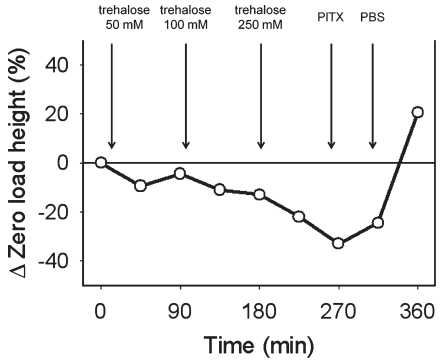

Figure 7. Analysis of the effect of trehalose on MCF-7 cells by AFM. Cells were incubated at 19 °C and subjected to indicated treatments. Graphical representation of the percentage variation of the zero load height related to incremental doses of trehalose. The height of the cells after stabilization under basal conditions was the reference value for the calculation of the percentage variations of those found in the course of the experiment. In the course of the experiment, the medium bathing the cells was replaced at the indicated times by complete culture medium containing trehalose at the final concentrations of 50 mM, 100 mM, and 250 mM, as specified. After the last medium change with the highest trehalose concentration, cells were further incubated for 90 min, and the solution bathing MCF-7 cells was then substituted with fresh medium devoid of trehalose and containing 0.3 nM PlTX. The toxin treatment continued for 45 min and was terminated by the substitution of the medium with PBS buffer and a further incubation for 45 min. The results represent the mean values of zero force height related to two cells for each time-point.

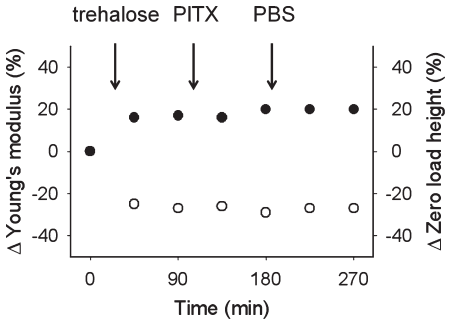

Figure 8. AFM analysis of the effect of trehalose on the damage induced by palytoxin in MCF-7 cells. Cells were incubated at 19 °C and received the culture medium containing 250 mM trehalose for 90 min. At the end of this reatment, the solution bathing MCF-7 cells was substituted with fresh medium devoid of trehalose and containing 0.3 nM PlTX and the incubation continued for 90 min. At the end of this incubation, the medium was exchanged for PBS started and the incubation continued for 90 min. The different treatments to the cells are indicated by arrows on the time scale. Plot of the percentage variation of the zero load height (empty symbols) and Young's modulus (closed symbols). The data result from an average of four cells for each time-point.

The data we obtained are reported in Figure 7 (the corresponding cell images are reported in Figures S12 and S13, in Supporting Information) and show that cells respond to increased concentrations of trehalose in culture medium by adjusting their volume. Trehalose, at a 50 mM final concentration, in fact, induces a decrease in cell height, but the compensatory process of relative volume increase[55] ensues, with a substantial recovery of cell height to control values (Figure 7). The detection of cell volume adjustment, however, was progressively blunted when cells were exposed to medium containing trehalose concentrations higher than 100 mM, under the time-scale of our experiment. In keeping with previous observations, the cell treatment with toxin, by substituting the solution bathing MCF-7 cells with fresh medium containing 0.3 nM PlTX but devoid of trehalose, induced a limited change in MCF-7 cell height, but a further substitution of incubation medium with PBS buffer induced a rapid return of cell height to basal levels (Figure 7).

On the basis of these observations, we next analyzed the protective effects that trehalose exerts on MCF-7 cells from the damages induced by PlTX using AFM and an experimental design taking into consideration that the protective effect can be observed when the osmolyte is present during the cell exposure to PlTX (Figure 3). Figure 8 reports the data we obtained (the corresponding cell images are reported in Figure S14 in Supporting Information). As expected, the addition of a medium containing such a high concentration of trehalose rapidly induced the shrinking of the cells, which is indicated by the decrease in cell height and the increase in its stiffness (the Young's modulus, Figure 8). When PlTX was added to the medium containing trehalose up to a final concentration of 0.3 nM, the height of the cells and their Young's modulus were not significantly affected. Under these conditions, the exchange of the medium for PBS did not induce detectable increases in cell height as opposed to the case in which the cells had been exposed to PlTX in the absence of trehalose (Figure 8). It is clear that the presence of trehalose in cell medium before and during PlTX treatment prevented the changes in mechanical properties induced by the toxin in MCF-7 cells.

Effects of Palytoxin on the Electrophysiological Properties of MCF-7 Cells. As a further approach to characterize the PlTX-induced cytolysis of MCF-7 cells, we applied patch-clamp recording techniques to monitor some electrophysiological properties that are linked to the ion imbalance occurring as a consequence of toxin interaction with the Na^+,K^+-ATPase.

In a first series of experiments, we tested whether input resistance (R_{in}) of MCF-7 cells was affected by PlTX under non-physiological temperature (20−25 °C) and suboptimal PlTX concentration (0.1 nM). These methodological choices were made to best approximate the experimental conditions of electrophysiological studies with those used in our preceding experiments, as described above, and to maximize their compatibility with the maintenance of proper functioning of cells subjected to patch-clamp recordings.

R_{in} is usually taken as an estimation of the cell membrane resistance in patch-clamp studies, that is, it represents an index for the presence of ion pathways. In fact, it is well known that PlTX increases the membrane conductance by transforming the Na^+,K^+-ATPase into a nonselective cation channel.[56−62] To confirm this effect, we monitored if PlTX affected R_{in} in our experimental model. Figure 9A shows sample records of currents from an MCF-7 cell before (control) and during PlTX application (PlTX). The increase in the current amplitude indicates a drop in R_{in}. This can be appreciated from the time course shown in Figure 9C. Data were normalized to the control values in order to monitor only the variation due to the toxin effect, thus avoiding possible differences in R_{in} among cells. It is possible to observe a remarkable drop in R_{in} by almost half of the control values just after 1 min of PlTX application.

Since in the original experiments on PlTX-induced cytolysis MCF-7 cells were incubated for 60 min with PlTX, we decided

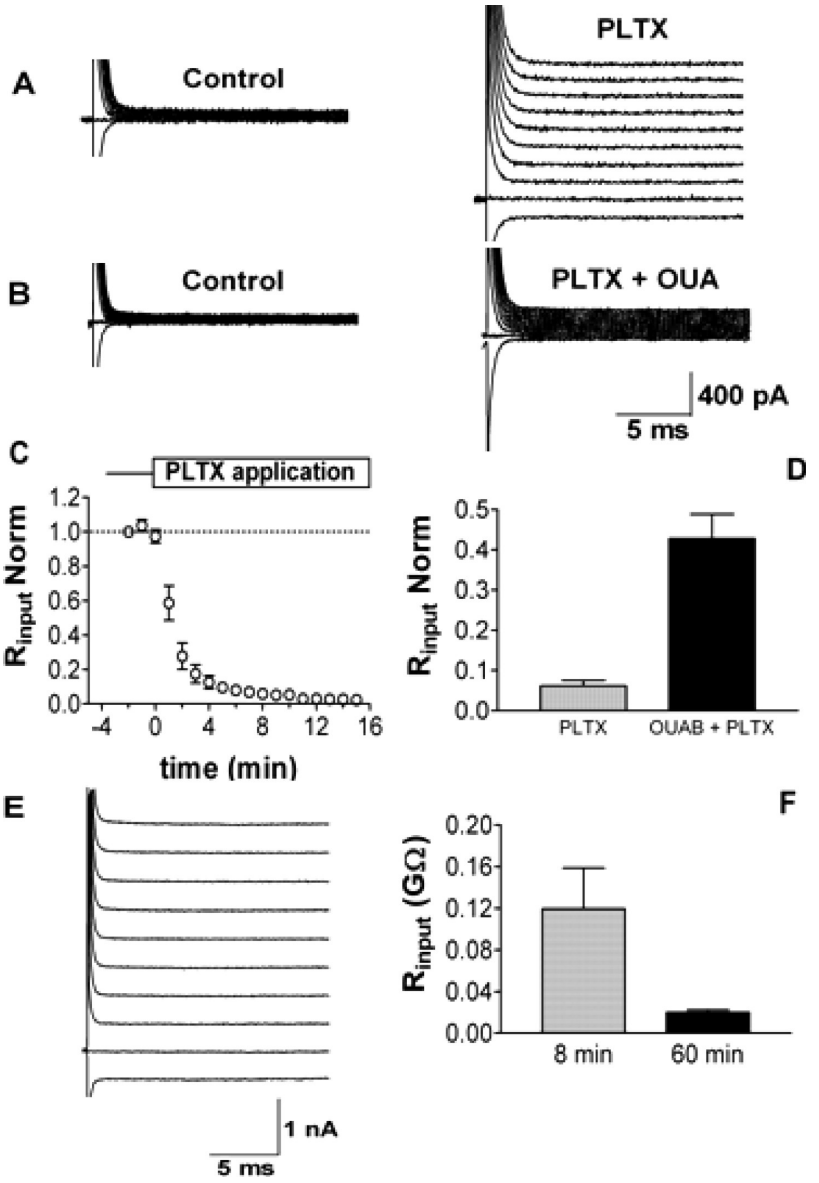

Figure 9. Effect of palytoxin on input resistance in MCF-7 cells. (Panel A) Patch-clamp recordings from a single MCF-7 cell held at −50 mV and stepped in 10-mV increments from −60 to 30 mV, under control conditions (left) and after 6 min of 0.1 nM PlTX bath-application (right). (Panel B) Patch-clamp recordings from a single MCF-7 cell (voltage protocol as in A) under control conditions (left) and after 6 min of 0.1 nM PlTX bath-application following 4 min of pretreatment with 100 μM ouabain (right). (Panel C) Time course of the effect of PlTX on R_{in}. Bath-application of 0.1 nM PlTX triggers a quick and huge drop in the normalized values of R_{in}. Points represent the mean value ± SEM ($n = 9$). (Panel D) Ouabain partially inhibits the action of PlTX on R_{in}. Pretreatment with 100 μM ouabain for 4 min partially blocks the action of 0.1 nM PlTX after 8 min of toxin exposure. Data of PlTX and OUAB + PlTX are from 13 and 6 MCF-7 cells, respectively. (Panel E) Patch-clamp recordings from a single MCF-7 cell (voltage protocol as in A) incubated for 60 min with 0.1 nM PlTX. (Panel F) A comparison between R_{in} values (means ± SEM) from MCF-7 cells after 8 and 60 min of exposure to 0.1 nM PlTX. Data of 8 and 60 min are from 12 and 14 MCF-7 cells, respectively.

to simulate this condition in electrophysiological experiments. This allowed us to find out the status of the cell membrane just before the switch of the culture medium to PBS, as performed in biochemical experiments. We then evaluated R_{in} in MCF-7 cells incubated for 60 min with PlTX before patch-clamping the cell membrane because it was not possible to hold the whole-cell recording for such long time. Figure 9E shows sample records of currents from an MCF-7 cell pretreated with toxin. A large increase in the current amplitude indicating a conspicuous drop in R_{in} can be noted. Figure 9F shows the mean values of R_{in} evaluated under these conditions and compared to the value obtained from nonpretreated cells after 8 min of toxin exposure. R_{in} data were not normalized in this analysis because it was not possible to have control values for the 60 min group, as explained above. It can be noted that R_{in} was further decreased by prolonging cell exposure to PlTX. Thus, the reduction of R_{in} induced by PlTX in MCF-7 cells is likely due to the transformation of Na^+,K^+-ATPase into ion channels, leading to a change in PNa/PK that shifts from 0.38 in control conditions to 0.77 after the cell exposure to the toxin (quantified as described in the Materials and Methods section).

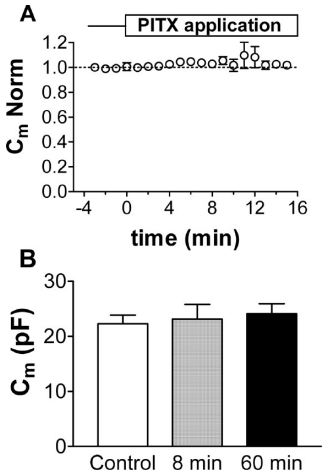

Figure 10. Effect of palytoxin on membrane capacitance in MCF-7 cells. (Panel A) PlTX (0.1 nM) does not affect normalized C_m of MCF-7 cells during 15 min of bath application (n = 8 cells). (Panel B) Comparison among C_m values (means ± SEM) in cells before PlTX treatment, after 8 and 60 min of exposure to 0.1 nM PlTX. Data were obtained from 16, 13, and 6 MCF-7 cells, respectively.

It has been shown that ouabain, an inhibitor of Na^+,K^+-ATPase, is able to reduce the effect of PlTX on the pump itself.[15,56] We then performed some experiments to evaluate whether the reduction in R_{in} induced by PlTX in MCF-7 cells was due to an action on Na^+,K^+-ATPase. Figure 9B shows sample records of currents from MCF-7 cells before (Control) and during PlTX application in the presence of ouabain (PlTX + OUA). In these experiments, cells were pretreated with ouabain (100 μM) alone for 4 min before applying the toxin. We chose this concentration of ouabain because it was shown to be the most effective in reducing the cytolytic effect of PlTX in MCF-7 cells.[23] As indicated by the small increase in the current amplitude, the decrease in R_{in} induced by PlTX was less pronounced when ouabain was present (compare records in panel A and B, on the right). Figure 9D summarizes data on the normalized R_{in} evaluated in cells treated with PlTX alone (left histogram) or in the presence of ouabain (right histogram). Ouabain clearly reduced the R_{in} drop due to PlTX, confirming that Na^+,K^+-ATPase is targeted by this toxin in MCF-7 cells. Overall, these results clearly show that our experimental system responds to PlTX and OUA by changes in electrophysiological properties which do not differ from those found in other models[15,59−62] and remains stable and capable to respond to PlTX even under suboptimal conditions.

We then evaluated the behavior of C_m in MCF-7 cells treated with 0.1 nM PlTX. C_m was taken as an index of the membrane surface area, and therefore, it can be used to electrophysiologically monitor possible variations of the membrane extension, which could accompany changes in cell volume. To the best of our knowledge, the effect of PlTX on C_m in isolated cells has not been reported so far. Figure 10A shows the effect of bath-applied PlTX on the value of C_m normalized to control values (points before PlTX application). Normalization was necessary to detect possible variations without taking into account the real size of the cells subjected to this treatment. Data indicated that C_m did not change significantly in the presence of PlTX during a period of 15 min.

As we did for R_{in} measurements, we carried out a set of experiments in which MCF-7 cells were incubated in the registration chamber over 60 min in the presence of 0.1 nM PlTX before recording. Figure 10B shows the mean values of C_m evaluated under these conditions and compared to the value obtained before PlTX treatment and after 8 min of toxin exposure. C_m data were not normalized in this analysis because it was not possible to have control values for the 60-min group, as explained above. It can be noted that C_m did not undergo any significant variation between the two different exposure times. As a whole, these results show that the C_m of MCF-7 cells was not affected by PlTX, indicating that the surface area of the cells was not significantly altered under our experimental conditions, in keeping with the limited change in cell volume detected by AFM.

DISCUSSION

In this investigation, we have integrated biochemical, morphological, physiological, and physical tools for the analysis of responses in MCF-7 cells exposed to PlTX. This integrated experimental approach and the use of suboptimal conditions for the induction of responses, such as lower toxin concentrations, nonphysiological temperatures of cell treatments, and modified/incomplete media for cell incubations, have allowed us to dissect some morphological features, steps, and mechanistic aspects of the cytolytic process induced by PlTX. The results we obtained show that PlTX causes a two-step cytolytic response in MCF-7 cells. The first phase of the response is toxin-dependent and osmolyte-sensitive, priming the cells to lytic events, taking place in a separate phase which does not require the presence of the toxin and is osmolyte-insensitive (Figures 1−3). The cytolytic response of MCF-7 cells has been shown to be inhibited by ouabain,[23] indicating that PlTX acts by impairing the functioning of Na^+,K^+-ATPase and then alters ion equilibria in MCF-7 cells. The data we obtained by patch-clamp recording confirmed existing data on the effects of PlTX on electrophysiological properties of cells after the toxin has converted the Na^+,K^+-ATPase into a cation channel[56−62] and the conclusion that this pump is targeted by PlTX in MCF-7 cells (Figure 9). Furthermore, the data obtained by patch-clamp recording show that the cytolytic response induced by the toxin involves an ion imbalance, without any detectable change in the surface area of the cells, as indicated by measurements of C_m in MCF-7 cells (Figure 10). Thus, cell swelling and excessive osmotic stress should not represent the driving force of the lytic events triggered by PlTX in MCF-7 cells under the conditions of this study.

This conclusion is further supported by the results we obtained when the morphology of MCF-7 cells was examined by AFM and immunofluorescence microscopy. Overall, the data obtained by immunofluorescence microscopy revealed that defined morphological changes can be detected in cells exposed to PlTX, including a slight decrease in the cross-sectional area of MCF-7 cells accompanied by a relative reorganization of the actin-based cytoskeleton in the peri-nuclear region of the cells (Figures 4,5). Other alterations in the shape of MCF-7 cells become visible by the use of AFM upon exposure to PlTX, after substitution of the toxin-containing medium for an isotonic buffer (PBS). In particular, the addition of PBS to MCF-7 cells that had been previously exposed to PlTX causes an increase in the height and volume of the cells, which is accompanied by a decreased stiffness (Young's modulus) at their surface (Figure 6, bottom panel). These alterations were prevented if a

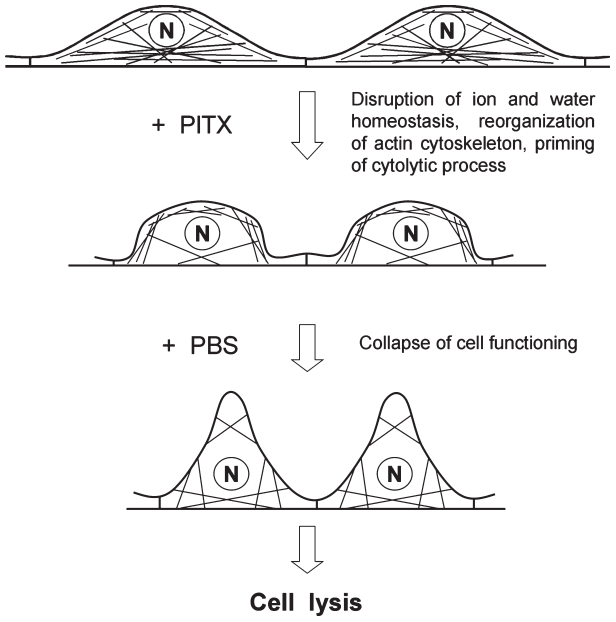

Figure 11. Working model of the cytolytic process triggered by PlTX in MCF-7 cells. The model has been derived by integrating the experimental data gathered by biochemical, immunological, physiological, and physical analyses carried out in our experimental system. The priming and execution phases leading to cytolysis induced by PlTX in MCF-7 cells are distinguished on the basis of key features of the experimental system, as described in the article. See text for explanations of the working model.

cell-impermeant osmolyte (trehalose) was present in the incubation medium during toxin treatment (Figure 8), implying that the events occurring in the first, osmolyte-sensitive phase of the process, eventually leading to morphological alterations of MCF-7 cell shape during the osmolyte-insensitive step, depend on the impairment of ion homeostasis caused by the toxin. Furthermore, the increase in the height and volume of PlTX-treated cells exposed to PBS was accompanied by a decrease in their stiffness, indicating that cell lysis involves a change in mechanical properties of the cells at their surface, which is not a direct consequence of membrane straining due to osmotic shock, in keeping with the observation that this second step of the process is osmolyte-insensitive. Furthermore, a reorganization of the actin-based cytoskeleton (Figure 4), accompanied by depolymerization of F-actin (Figure 5), occurs in MCF-7 cells exposed to PlTX, suggesting that this response could have a role in the decreased stiffness of PlTX-treated cells at their surface (Figure 6). Thus, cell lysis could result from plasma membrane rupture in cells lacking a proper mechanical scaffolding at their surface, as a consequence of PlTX action.

A working model of the cytolytic process triggered by PlTX in our experimental system, based on the entire set of findings described in this report, is outlined in Figure 11. The effect of PlTX is triggered by impairing the Na^+,K^+-ATPase and the consequent alteration of ion and water homeostasis in MCF-7 cells (Figures 1−3, 9, and 10). A 60−90 min treatment of MCF-7 cells with PlTX does not result in significant changes of cell volume and cell height (Figure 6) but is sufficient to prime cytolysis, which rapidly ensues when cells are exposed to unfavorable conditions, such as incubation with an isotonic buffer devoid of nutrients present in a complete culture medium (Figures 1,3). PlTX induces alterations of the MCF-7 cell morphology, including a rearrangement of the actin-based cytoskeleton, which is accompanied by a relative decrease in the cross-sectional area of the cells, without any gross impairment of cell−cell adhesion (Figures 4,5, and Figures S7,S8 in Supporting Information). These changes in the cell's architecture proceed with an osmolyte-insensitive increase of cell height and volume, and culminate with cell lysis (Figures 6,8). The decrease in the Young's modulus detected in the lytic phase of the process implies a decreased stiffness of the plasma membrane and an increased susceptibility to deformation of PlTX-treated cells exposed to PBS (Figure 6, bottom panel), which would be a consequence of the rearrangement of the actin-based cytoskeleton and its reorganization around nuclei (Figures 4,5,11). Cell lysis would then represent the most favored event in cells displaying altered cytoskeletal scaffolding and impaired mechanical properties at their surface.

Taken as a whole, the data we obtained show that the first phase of the lytic process is accompanied by limited morphological alterations in PlTX-treated cells, which further develop in the second phase and culminate in cell lysis (Figure 11). Although we have no direct proof of a cause−effect relationship between the morphological alterations we recorded and cell lysis, it seems likely that the first ones are part of the molecular events leading to MCF-7 cell lysis.

The mechanistic details of the priming and execution phases of the PlTX-induced cytolytic process in MCF-7 cells remain to be clarified. The available information regarding the molecular responses induced by PlTX in several systems, including MCF-7 cells, however, would suggest a working model[20] including several modules. In particular, the activation of p38 protein kinases,[63,64] a cell stress response characterized by the covalent modification of stress proteins,[41] the alteration of the actin-based cytoskeleton (reviewed in ref 65) would be induced by PlTX, culminating with the collapse of cell functioning and cell lysis. In this working hypothesis, the activation of p38 protein kinase[63,64] and of cell stress response[41] could represent key features of the priming, osmolyte-sensitive phase of the cytolytic process triggered by PlTX, whereas the alteration of the actin-based cytoskeleton could be part of the following osmolyte-insentive execution phase of the response induced by PlTX. In keeping with this working hypothesis, osmotic stresses have been found to activate p38 kinase in different biological systems,[66,67] and the activation of p38 protein kinases and the phosphorylation of hsp 27 have been shown to alter the actin-based cytoskeleton in cellular systems.[68]

Further studies are needed to fully clarify the mechanistic features of the cytolytic response induced by PlTX and its role in the toxic effects the toxin exerts in excitable and nonexcitable tissues. The characteristics of the process emerging from this study and the identification of experimental conditions allowing the dissection of steps in the response, as well as their manipulation, could provide a useful experimental model for further studies on the molecular bases of PlTX actions and the clarification of its pleiotropic effects *in vivo*.

■ ASSOCIATED CONTENT

Supporting Information. Results obtained in complementary biochemical, immunofluorescence, and AFM analyses of PlTX effects on MCF-7 cells. This material is available free of charge via the Internet at http://pubs.acs.org.

AUTHOR INFORMATION

Corresponding Author

*E-mail: gianpaolo.rossini@unimore.it.

Funding Sources

This investigation was supported by the Italian Ministero dell'Istruzione, dell'Università e della Ricerca.

ACKNOWLEDGMENT

We thank Aurélie Ledreux for her critical comments on our investigations, which stimulated constructive discussions.

REFERENCES

(1) Moore, R. E., and Scheuer, P. J. (1971) Palytoxin: a new marine toxin from a coelenterate. *Science 172*, 495–498.

(2) Kimura, S., Hashimoto, Y., and Yamazato, K. (1972) Toxicity of the zoanthid *Palythoa tuberculosa*. *Toxicon 10*, 611–617.

(3) Onuma, Y., Satake, M., Ukena, T., Roux, J., Chanteau, S., Rasolofonirina, N., Ratsimaloto, M., Naoki, H., and Yasumoto, T. (1999) Identification of putative palytoxin as the cause of clupeotoxism. *Toxicon 37*, 55–65.

(4) Lenoir, S., Ten-Hage, L., Turquet, J., Quod, J. P., Bernard, C., and Hennion, M. C. (2004) First evidence of palytoxin analogues from an *Ostreopsis mascarenensis* (Dinophyceae) benthic bloom in Southwestern Indian Ocean. *J. Phycol. 40*, 1042–1051.

(5) Ciminiello, P., Dell'Aversano, C., Fattorusso, E., Forino, M., Magno, S., Tartaglione, L., Grillo, C., and Melchiore, N. (2006) The Genoa 2005 outbreak. Determination of palytoxin in Mediterranean *Ostreopsis ovata* by a new liquid chromatography tandem mass spectrometry method. *Anal. Chem. 78*, 6153–6159.

(6) Ciminiello, P., Dell'Aversano, C., Fattorusso, E., Forino, M., Tartaglione, L., Grillo, C., and Melchiorre, N. (2008) Putative palytoxin and its new analogue, ovatoxin-a, in *Ostreopsis ovata* collected along the Ligurian coasts during the 2006 toxic outbreak. *J. Am. Soc. Mass Spectrom. 19*, 111–120.

(7) Moore, R. E., and Bartolini, G. (1981) Structure of palytoxin. *J. Am. Chem. Soc. 103*, 2491–2494.

(8) Uemura, D., Ueda, K., Hirata, Y., Naoki, H., and Iwashita, T. (1981) Further studies on palytoxin.1. *Tetrahedron Lett. 22*, 1909–1912.

(9) Uemura, D., Ueda, K., Hirata, Y., Naoki, H., and Iwashita, T. (1981) Further studies on palytoxin. 2. Structure of palytoxin. *Tetrahedron Lett. 22*, 2781–2784.

(10) Deeds, J. R., and Schwartz, M. D. (2010) Human risk associated with palytoxin exposure. *Toxicon 56*, 150–162.

(11) Tubaro, A., Durando, P., Del Favero, G., Ansaldi, F., Icardi, G., Deeds, J. R., and Sosa, S. (2011) Case definitions for human poisonings postulated to palytoxins exposure. *Toxicon 57*, 478–495.

(12) Rossini, G. P., and Hess, P. (2009) Phycotoxins: Chemistry, Mechanisms of Action and Shellfish Poisoning, in *Molecular, Clinical and Environmental Toxicology* (Luch, A., Ed.), pp 65−122, Birkhåuser-Verlag AG, Basel, Switzerland.

(13) Mangialajo, L., Ganzin, N., Accoroni, S., Asnaghi, V., Blanfuné, A., Cabrini, M., Cattaneo-Vietti, R., Chavanon, F., Chiantore, M., Cohu, S., Costa, E., Fornasaro, D., Grossel, H., Marco-Miralles, F., Masó, M., Reñé, A., Rossi, A. M., Sala, M. M., Thibaut, T., Totti, C., Vila, M., and Lemée, R. (2011) Trends in *Ostreopsis* proliferation along the Northern Mediterranean coasts. *Toxicon 57*, 408–420.

(14) Gallitelli, M., Ungaro, N., Addante, L. M., Gentiloni, N., and Sabbà, C. (2005) Respiratory illness as a reaction to tropical algal blooms occurring in a temperate climate. *JAMA 293*, 2599–2600.

(15) Habermann, E., and Chhatwal, G. S. (1982) Ouabain inhibits the increase due to palytoxin of cationic permeability of erythrocytes. *Naunyn-Schmeideberg's Arch. Pharmacol. 319*, 101–107.

(16) Gadsby, D. C., Takeuchi, A., Artigas, P., and Reyes, N. (2009) Peering into an ATPase ion pump with single channel recordings. *Phil. Trans. R. Soc. B 364*, 229–238.

(17) Wu, C. H. (2009) Palytoxin: Membrane mechanism of action. *Toxicon 54*, 1183–1189.

(18) Rossini, G. P., and Bigiani, A. (2011) Palytoxin action on the Na^+,K^+-ATPase and the disruption of ion equilibria in biological systems. *Toxicon 57*, 429–439.

(19) Habermann, E. (1989) Palytoxin acts through Na^+, K^+-ATPase. *Toxicon 27*, 1171–1187.

(20) Bellocci, M., Sala, G. L., and Prandi, S. (2011) The cytolytic and cytotoxic activities of palytoxin. *Toxicon 57*, 449–459.

(21) Habermann, E., Ahnert-Hilger, G., Chhatwal, G. S., and Beress, L. (1981) Delayed haemolytic action of palytoxin general characteristics. *Biochim. Biophys. Acta 649*, 481–486.

(22) Bignami, G. S. (1993) A rapid and sensitive hemolysis neutralization assay for palytoxins. *Toxicon 31*, 817–820.

(23) Bellocci, M., Ronzitti, G., Milandri, A., Melchiorre, N., Grillo, C., Poletti, R., Yasumoto, T., and Rossini, G. P. (2008) A cytolytic assay for the measurement of palytoxin based on a cultured monolayer cell line. *Anal. Biochem. 374*, 48–55. An addendum has appeared in *380*, 178.

(24) Cañete, E., and Diogène, J. (2008) Comparative study of the use of neuroblastoma cells (Neuro-2a) and neuroblastoma × glioma hybrid cells (NG108−15) for the toxic effect quantification of marine toxins. *Toxicon 52*, 541–550.

(25) Riobó, P., Paz, B., Franco, J. M., Vázquez, J., and Murado, M. A. (2008) Proposal for a simple and sensitive haemolytic assay for palytoxin. Toxicological dynamics, kinetics, ouabain inhibition and thermal stability. *Harmful Algae 7*, 415–429.

(26) Ledreux, A., Krys, S., and Bernard, C. (2009) Suitability of the Neuro-2a cell line for the detection of palytoxin and analogues (neurotoxic phycotoxins). *Toxicon 53*, 300–308.

(27) Malaguti, C., and Rossini, G. P. (2002) Recovery of cellular E-cadherin precedes replenishment of estrogen receptor and estrogen-dependent proliferation of breast cancer cells rescued from a death stimulus. *J. Cell. Physiol. 192*, 171–181.

(28) Wróblewski, F., and LaDue, J. S. (1956) Serum glutamic pyruvic transaminase in cardiac and hepatic disease. *Proc. Soc. Exp. Biol. Med. 91*, 569–571.

(29) Butt, H. J., and Jaschke, M. (1995) Calculation of thermal noise in atomic force microscopy. *Nanotechnology 6*, 1–7.

(30) Alessandrini, A., and Facci, P. (2005) AFM: a versatile tool in biophysics. *Measurement Sci. Technol. 16*, R65–R92.

(31) Hertz, H. (1882) Ueber die Berührung fester elasticher körper. *Reine Angew. Mathematik 92*, 156–171.

(32) Radmacher, M., Fritz, M., Kacher, C. M., Cleveland, J. P., and Hansma, P. K. (1996) Measuring the viscoelastic properties of human platelets with the atomic force microscope. *Biophys. J. 70*, 556–567.

(33) Domke, J., and Radmacher, M. (1998) Measuring the elastic properties of thin polymer films with the atomic force microscope. *Langmuir 14*, 3320–3325.

(34) Plesnila, N., Müller, E., Guretzki, S., Ringel, F., Staub, F., and Baethmann, A. (2000) Effect of hypothermia on the volume of rat glial cells. *J. Physiol. 523*, 155–162.

(35) Sunyer, R., Trepat, X., Fredberg, J. J., Farré, R., and Navajas, D. (2009) The temperature dependence of cell mechanics measured by atomic force microscopy. *Phys. Biol. 6*, 25009.

(36) Hamill, O. P., Marty, A., Neher, E., Sakmann, B., and Sigworth, F. J. (1981) Improved patch-clamp techniques for high-resolution current recording from cells and cell-free membrane patches. *Pflugers Arch. 391*, 85–100.

(37) Klimatcheva, E., and Wonderlin, W. F. (1999) An ATP-sensitive K^+ current that regulates progression through early G1 phase of the cell cycle in MCF-7 human breast cancer cells. *J. Membr. Biol. 171*, 35–46.

(38) Ouadid-Ahidouch, H., Chaussade, F., Roudbaraki, M., Slomianny, C., Dewailly, E., Delcourt, P., and Prevarskaya, N. (2000) KV1.1 K^+ channels identification in human breast carcinoma cells: involvement in cell proliferation. *Biochem. Biophys. Res. Commun. 278*, 272–277.

(39) Gillis, K. D. (1995) Techniques for Membrane Capacitance Measurements, in *Single-Channel Recording* (Sakmann, B., and Neher, E., Eds.) pp 155−197, Plenum Press, New York.

(40) Hille, B. (2001) *Ion Channels of Excitable Membranes*, Sinauer Associates, Sunderland, MA.

(41) Sala, G. L., Bellocci, M., and Rossini, G. P. (2009) The cytotoxicity pathway triggered by palytoxin involves a change in the cellular pool of stress response proteins. *Chem. Res. Toxicol. 22*, 2009–2016.

(42) Horowitz, S. B., and Fenichel, I. R. (1968) Analysis of glycerol-^{3}H transport in frog oocyte by extractive and radioautographic techniques. *J. Gen. Physiol. 51*, 703–730.

(43) Rossini, G. P., and Malaguti, C. (1994) Nanomolar concentrations of untransformed glucocorticoid receptor in nuclei of intact cells. *J. Steroid Biochem. Mol. Biol. 51*, 291–298.

(44) Nollet, F., Kools, P., and van Roy, F. (2000) Phylogenetic analysis of the cadherin superfamily allows identification of six major subfamilies besides several solitary members. *J. Mol. Biol. 299*, 551–572.

(45) Bellocci, M., Sala, G. L., Callegari, F., and Rossini, G. P. (2010) Azaspiracid-1 inhibits endocytosis of plasma membrane proteins in epithelial cells. *Toxicol. Sci. 117*, 109–121.

(46) Ares, I. R., Cagide, E., Louzao, M. C., Espina, B., Vieytes, M. R., Yasumoto, T., and Botana, L. M. (2009) Ostreocin-D impact on globular actin of intact cells. *Chem. Res. Toxicol. 22*, 374–81.

(47) Löw, I., Dancker, P., and Wieland, T. (1975) Stabilization of F-actin by phalloidin. reversal of the destabilizing effect of cytochalasin B. *FEBS Lett. 54*, 263–265.

(48) Schneider, S. W., Yano, Y., Sumpio, B. E., Jena, B. P., Geibel, J. P., Gekle, M., and Oberleithner, H. (1997) Rapid aldosterone-induced cell volume increase of endothelial cells measured by the atomic force microscope. *Cell Biol. Int. 21*, 759–768.

(49) Rotsch, C., and Radmacher, M. (2000) Drug-induced changes of cytoskeletal structure and mechanics in fibroblasts: an atomic force microscopy study. *Biophys. J. 78*, 520–535.

(50) Smith, B. A., Tolloczko, B., Martin, J. G., and Grütter, P. (2005) Probing the viscoelastic behavior of cultured airway smooth muscle cells with atomic force microscopy: stiffening induced by cantractile agonist. *Biophys. J. 88*, 2994–3007.

(51) Hillebrand, U., Hausberg, M., Lang, D., Stock, C., Riethmüller, C., Callies, C., and Büssemaker, E. (2008) How steroid hormones act on the endothelium: insights by atomic force microscopy. *Pflugers Arch. 456*, 51–60.

(52) Pelling, A. E., Dawson, D. W., Carreon, D. M., Christiansen, J. J., Shen, R. R., Teitell, M. A., and Gimzewski, J. K. (2007) Distinct contributions of microtubule subtypes to cell membrane shape and stability. *Nanomedicine 3*, 43–52.

(53) Oberleithner, H., Callies, C., Kusche-Vihrog, K., Schillers, H., Shahin, V., Riethmüller, C., Macgregor, G. A., and de Wardener, H. E. (2009) Potassium softens vascular endothelium and increases nitric oxide release. *Proc. Natl. Acad. Sci. U.S.A. 106*, 2829–2834.

(54) Li, Q. S., Lee, G. Y. H., Ong, C. N., and Lim, C. T. (2008) AFM indentation study of breast cancer cells. *Biochem. Biophys. Res. Commun. 374*, 609–613.

(55) Hoffmann, E. K., Lambert, I. H., and Pedersen, S. F. (2009) Physiology of cell volume regulation in vertebrates. *Physiol. Rev. 89*, 193–277.

(56) Chhatwal, G. S., Hessler, H. J., and Habermann, E. (1983) The action of palytoxin on erythrocytes and resealed ghosts. Formation of small, nonselective pores linked with Na^+, K^+-ATPase. *Naunyn-Schmiedeberg's Arch. Pharmacol. 323*, 261–268.

(57) Muramatsu, I., Uemura, D., Fujiwara, M., and Narahashi, T. (1984) Characteristics of palytoxin-induced depolarization in squid axons. *J. Pharmacol. Exp. Ther. 231*, 488–494.

(58) Muramatsu, I., Nishio, M., Kigoshi, S., and Uemura, D. (1988) Single ionic channels induced by palytoxin in guinea-pig ventricular myocytes. *Br. J. Pharmacol. 93*, 811–816.

(59) Ikeda, M., Mitani, K., and Ito, K. (1988) Palytoxin induces a nonselective cation channel in single ventricular cells of rat. *Naunyn-Schmeideberg's Arch. Pharmacol. 337*, 591–593.

(60) Scheiner-Bobis, G., Meyer zu Heringdorf, D., Christ, M., and Habermann, E. (1994) Palytoxin induces K^+ efflux from yeast cells expressing the mammalian sodium pump. *Mol. Pharmacol. 45*, 1132–1136.

(61) Redondo, J., Fiedler, B., and Scheiner-Bobis, G. (1996) Palytoxin-induced Na^+ influx into yeast cells expressing the mammalian sodium pump is due to the formation of a channel within the enzyme. *Mol. Pharmacol. 49*, 49–57.

(62) Hirsh, J. K., and Wu, C. H. (1997) Palytoxin-induced single-channel currents from the sodium pump synthesized by in vitro expression. *Toxicon 35*, 169–176.

(63) Li, S., and Wattenberg, E. V. (1998) Differential activation of mitogen-activated protein kinases by palytoxin and ouabain, two ligands for the Na^+, K^+-ATPase. *Toxicol. Appl. Pharmacol. 151*, 377–384.

(64) Li, S., and Wattenberg, E. V. (1999) Cell-type-specific activation of p38 protein kinase cascades by the novel tumor promoter palytoxin. *Toxicol. Appl. Pharmacol. 160*, 109–119.

(65) Louzao, M. C., Ares, I. R., Cagide, E., Espiña, B., Vilariño, N., Alfonso, A., Vieytes, M. R., and Botana, L. M. (2011) Palytoxins and cytoskeleton: an overview. *Toxicon 57*, 460–469.

(66) Tilly, B. C., Gaestel, M., Engel, K., Edixhoven, M. J., and de Jonge, H. R. (1996) Hypo-osmotic cell swelling activates the p38 MAP kinase signalling cascade. *FEBS Lett. 395*, 133–136.

(67) Zhang, Z., and Cohen, D. M. (1996) NaCl but not urea activates p38 and jun kinase in mIMCD3 murine inner medullary cells. *Am. J. Phisiol. 271*, F1234–F1238.

(68) Mounier, N., and Arrigo, A.-P. (2002) Actin cytoskeleton and small heat shock proteins: how do they interact?. *Cell Stress Chaperones 7*, 167–176.